BJP BRITISH JOURNAL OF PHARMACOLOGY

BPS BRITISH PHARMACOLOGICAL SOCIETY

BJP British Journal of Pharmacology

DOI:10.1111/j.1476-5381.2010.01047.x
www.brjpharmacol.org

RESEARCH PAPER

Rimonabant reduces keratinocyte viability by induction of apoptosis and exerts topical anti-inflammatory activity in mice

Anna Maria Malfitano[1], Silvio Sosa[2], Chiara Laezza[3], Marco De Bortoli[2], Aurelia Tubaro[2] and Maurizio Bifulco[1]

[1]*Department of Pharmaceutical Sciences, University of Salerno, Fisciano, Salerno, Italy,*
[2]*Department of Materials and Natural Resources, University of Trieste, Trieste, Italy, and*
[3]*Department of Biologia and Patol. Cell. Mol. and Institute of Endocrinology and Experimental Oncology, IEOS, CNR, Naples, Italy*

Correspondence
Prof Maurizio Bifulco, Department of Pharmaceutical Sciences, University of Salerno, Via Ponte don Melillo, 84084 Fisciano, Salerno, Italy. E-mail: mbifulco@unisa.it

Keywords
cannabinoid receptor CB1; CB1 antagonist; keratinocytes; cell viability; apoptosis; dermatitis; oedema; leukocyte infiltrate

Received
27 April 2010
Revised
16 July 2010
Accepted
22 July 2010

BACKGROUND AND PURPOSE

There is growing evidence that the cannabinoid CB_1 receptor antagonist, rimonabant (SR141716) exerts potential anti-proliferative and anti-inflammatory actions. Here, we have assessed the effects of rimonabant *in vitro* in murine immortalized keratinocytes and *in vivo* by assaying the topical anti-inflammatory activity.

EXPERIMENTAL APPROACH

Cell viability and death in a keratinocyte cell line (C5N cells) were measured by Trypan blue exclusion assay and cytotoxicity by sulphorhodamine B test. Cell cycle progression was assessed by flow cytometry and the expression of apoptotic and anti-apoptotic markers, cyclins, pathways of signal transduction and CB1 receptor levels were evaluated by Western blot. The topical anti-inflammatory properties of rimonabant were analysed by inhibition of croton oil-induced ear dermatitis in mice.

KEY RESULTS

Rimonabant reduced cell viability and induced apoptosis as shown by the enhanced number of cells in the subG0 phase of the cell cycle, the expression of Bax and reduced levels of Bcl-2 and X-inhibitor of apoptosis protein. In addition, reduced levels of phosphorylated serine/threonine protein kinase Akt and nuclear factor-kappa B were detected associated with regulation of total nuclear factor-kappa B and inhibitor of kappa B-α, phosphorylated inhibitor of kappa B-α, cyclins D1, E and A. In croton oil-induced ear dermatitis, rimonabant significantly reduced oedema and leukocyte infiltrate.

CONCLUSIONS AND IMPLICATIONS

Rimonabant reduced cell viability, inducing cell death in keratinocytes and decreased croton oil-induced ear dermatitis. Our findings suggest a potential application of rimonabant as a topical anti-inflammatory drug. We did not assess the involvement of CB_1 receptors in these effects of rimonabant.

Abbreviations

FBS, fetal bovine serum; NSAID, non-steroidal anti-inflammatory drug; TMB, tetramethylbenzidine; TRPV1, vanilloid receptor

Introduction

Rimonabant (SR141716) [N-piperidino-5-(4-chlorophenyl)-1-(2,4-dichlorophenyl)-4methyl pyrazole-3-carboxamide] is a potent and selective cannabinoid CB_1 receptor antagonist (receptor nomenclature follows Alexander *et al.*, 2009), inhibiting food intake and exhibiting anti-obesity activity (Rinaldi-Carmona *et al.*, 1994; 1995; Colombo *et al.*, 1998; Simiand *et al.*, 1998; Ravinet Trillou *et al.*, 2003; Carai *et al.*, 2005; Jbilo *et al.*, 2005). It is widely used as a tool to investigate mechanisms by which cannabinoid agonists produce their pharmacological effects and may exert several of its actions by blocking the activation of CB_1 receptors, thus modulating the endocannabinoid system, which is tonically activated under certain pathophysiological conditions (Di Marzo and Matias, 2005; Engeli *et al.*, 2005; Matias *et al.*, 2006; Jhaveri *et al.*, 2007; Pertwee, 2009). Anti-tumour properties have been attributed to rimonabant by our group in several cancer cell lines *in vitro* and *in vivo* (Sarnataro *et al.*, 2006; Santoro *et al.*, 2008; 2009; Gazzerro *et al.*, 2010). Nonetheless, we very recently provided evidence that rimonabant increases human sperm motility and viability (Aquila *et al.*, 2010). Numerous findings suggested the role of the endocannabinoid system in the control of immunity, reporting the involvement of cannabinoid receptors in immune cell migration (Miller and Stella, 2008) and the efficacy of cannabinoid agonists as antinociceptive and anti-inflammatory agents (Guindon and Hohmann, 2008). We recently demonstrated the immunomodulatory and anti-inflammatory effects of rimonabant on peripheral blood mononuclear cells, showing inhibition of proliferation without induction of apoptosis, block of the G1/S phase of the cell cycle and modulation of the signalling kinases serine/threonine protein kinase Akt (Akt) and the extracellular signal regulated kinase, the transcription factor nuclear factor-kappa B (NF-κB) and its inhibitor (IκB) and the inducible enzymes cyclooxygenase-2 and inducible NO synthase (Malfitano *et al.*, 2008). In rats and mice, rimonabant prevents the rise in tumour necrosis factor-α (TNF-α) serum levels induced by *Escherichia coli* lipopolysaccharide and relieves neuropathic pain (Smith *et al.*, 2000; Costa *et al.*, 2005).

Other findings suggest a variety of mechanisms of action of rimonabant in the modulation of the inflammatory process. Oral administration of rimonabant dose-dependently prevented indomethacin-induced small intestinal ulcers in rats and inhibited TNF-α levels. However, in CB_1 receptor knockout mice, protection against ulcers was lost but TNF-α levels were still inhibited (Croci *et al.*, 2003). Furthermore, rimonabant reduced joint inflammation in a chronic model of adjuvant-induced unilateral arthritis in obese rats and inhibited thermal and mechanical hyperalgesia (Croci and Zarini, 2007). Recent intriguing findings have identified the functional existence of various members of the endocannabinoid system in human and murine skin (Maccarrone *et al.*, 2003; Ibrahim *et al.*, 2005; Ständer *et al.*, 2005). Cannabinoids suppressed *in vitro* proliferation of cultured epidermal keratinocytes (Ibrahim *et al.*, 2005; Paradisi *et al.*, 2008). In addition, using mice with the double CB_1/CB_2 receptor knockout, Karsak *et al.* (2007) elegantly demonstrated that endocannabinoids attenuated allergic contact dermatitis.

The aim of this study was to assess the effects of rimonabant *in vitro* in murine immortalized keratinocytes and *in vivo* to evaluate its topical anti-inflammatory activity, using an acute model of inflammation. Our results showed reduced cell viability and induction of apoptosis accompanied by regulation of phosphorylated protein kinase Akt (pAkT), NF-κB (pNF-κB) IκBα (pIκBα) and cyclins D1, E and A. In addition, rimonabant up-regulated the expression of CB_1 receptors and *in vivo*, inhibited croton oil-induced ear dermatitis in mice, reducing oedema and leukocyte infiltrate.

Methods

Cell growth and culture

C5N, a murine immortalized non-tumorigenic keratinocyte cell line (Portella *et al.*, 1998), supplied by Professor G. Portella (Federico II University of Naples) was used in this study. C5N cells were grown at 37°C in a humidified atmosphere of 5% CO_2 in Dubelco's Modified Eagle Medium (DMEM) culture medium supplemented with 10% heat inactivated fetal bovine serum (FBS) and glutamine (2 mM). Cells were starved by serum deprivation overnight before each assay.

Cell viability assay

Exponentially proliferating cells (1×10^5) were seeded in 24-well plates. Increasing concentrations of rimonabant (0.3 μM, 1 μM, 3 μM, 10 μM) were added to the culture. After 24 h and 48 h of incubation, cells were harvested, stained with Trypan blue (0.5% solution; Sigma) and counted by haemocytometer.

Cytotoxicity assay

C5N cells (1×10^5) were incubated 24 h in 96-well plates at the concentrations of rimonabant shown above. Cell monolayers were fixed with 10% (wt·vol^{-1}) trichloroacetic acid, stained for 30 min with sulphorhodamine B (0,4% in acetic acid) and then the excess dye was removed by washing repeatedly with 1% (vol vol^{-1}) acetic acid. The protein-bound dye was dissolved in 10 mM Tris base solution for optical density determination at 495 nm using a microplate reader.

Cell cycle analysis

C5N cells (10^5) were cultured in the presence and in the absence of rimonabant at the concentrations shown above, in DMEM 10% FBS for 24 h and 48 h at 37°C in 24-well plates. To analyse cell cycle progression, cells starved overnight in DMEM medium in the absence of FBS were collected, washed twice with phosphate-buffered saline (PBS) and re-suspended in 300 μL of PBS; 700 μL of 70% ethanol were added slowly to the cells on a vortex mixer and kept at –20°C for 1 h. Propidium iodide (PI; 10 μg·mL^{-1}) in PBS containing 100 U·mL^{-1} DNase-free RNase was added to the cells; after 15 min at room temperature, cells were subjected to flow cytometric analysis using Summit v4.3 program. Each sample was analysed using 10 000 events corrected for debris and aggregate populations.

Electrophoresis and immunoblots

Cell extracts were prepared from C5N cells. Cells were treated with rimonabant at 0.3 μM, 1 μM, 3 μM and 10 μM. After

24 h and 48 h of incubation, cells were washed twice with PBS, re-suspended in lysis buffer (50 mM HEPES, 150 mM NaCl, 50 mM EDTA, 100 mM NaF, 2 mM Na orthovanadate, glycerol, 10 mM $Na_4P_2O_7$ and 10% Triton at pH 7.5) and passed through a 23-gauge needle, 10 times before centrifugation at 12 000 g at 4°C. Supernatants were collected and the protein concentration evaluated by the Bradford method (Bradford, 1976). Equal amounts of protein extracts (50 µg) were boiled in sample buffer and analysed by electrophoresis in 12% sodium dodecylsulphate polyacrylamide gel, separated proteins were transferred to nitrocellulose membranes (Amersham Hybond ECL, Amersham GE Healthcare, Buckinghamshire, UK) (8 V for 1 h). The blots were blocked in PBS containing 0.1% Tween-20 and 5% non-fat dry milk for 1 h at room temperature. The membrane was then probed overnight with primary antibodies (1:1000) (host species : rabbit) specific for NF-κB p65 (Cell Signaling Technology Inc., Danvers, MA, USA) and its phosphorylated form, pNF-κB p65 (Cell signalling), IκBα (Cell signalling), pIκBα (Cell signalling), Bax (Santa Cruz Biotechnology Inc., Santa Cruz, CA, USA), Bcl-2 (Santa Cruz Biotechnology Inc.), the X-inhibitor of apoptosis protein (XIAP) (BD Transduction Laboratories, Franklin Lakes, NJ, USA), pAkt (Cell signalling), Akt (Cell signalling), cyclin (Cyc) D1 (Santa Cruz Biotechnology Inc.), Cyc E (Santa Cruz Biotechnology Inc.), Cyc A (Santa Cruz Biotechnology Inc.) and CB_1 receptors (Santa Cruz Biotechnology Inc.). Immunodetection of specific proteins was carried out with horseradish peroxidase-conjugated donkey anti-rabbit IgG (Bio-Rad, Life Science Research, Hercules, CA, USA), using the enhanced chemiluminescence system (Amersham GE Healthcare). Actin (Santa Cruz Biotechnology Inc., anti-rabbit) as control was used to normalize.

Topical anti-inflammatory activity in vivo

Croton oil induced ear dermatitis. All animal care and experimental procedures complied with the Italian D.L. no. 116 of January 27, 1992 and associated guidelines in the European Communities Council Directive of November 24, 1986 (86/609 ECC). Male CD-1 mice (Harlan Italy; S. Pietro al Natisone, Italy) were anaesthetized by intraperitoneal injection of ketamine hydrochloride (145 $mg \cdot kg^{-1}$). Skin inflammation was induced on their right ear (surface: about 1 cm^2) applying 80 µg of croton oil dissolved in 15 µL of acetone. The left ear remained untreated as preliminary experiments showed that the vehicle did not affect the inflammatory response or induce irritation. Control mice received only the irritant while other mice received the irritant and rimonabant or the non-steroidal anti-inflammatory drug (NSAID) indomethacin, used as reference. Mice were killed by cervical dislocation 6 h or 24 h after the induction of inflammation, at the times of maximum oedema response and leukocyte infiltrate in control mice respectively. Disks (6 mm diameter) were punched out of the ear to quantify the oedematous response and leukocyte infiltrate (Tubaro *et al.*, 1985). A total of 10 animals were used for each group of treatment.

Evaluation of the oedematous response. Oedema was quantified by the difference in weight between the samples taken from the right treated and left untreated ears. The anti-oedema activity was expressed as percent inhibition of oedema in mice treated with the test substances with respect to oedema of animals treated with the irritant alone (Tubaro *et al.*, 1985).

Evaluation of the granulocyte infiltrate. The cellular infiltrate was quantified in the treated ears measuring the myeloperoxidase activity, as index of the presence of neutrophilic granulocytes, in the same ear samples as used to determine oedema (Tubaro *et al.*, 1985). Myeloperoxidase was extracted by hexadecyltrimehylammonium bromide (HTAB; Sigma-Aldrich, Milan, Italy), according to Bradley *et al.* (1982), and the enzyme activity was measured by a colorimetric assay using tetramethylbenzidine (TMB; Sigma-Aldrich, Milan, Italy) as chromogen (Andrews and Krinsky, 1981). Each ear sample, suspended in 1 mL buffered saline (0.1 M sodium acetate buffer at pH 4.2), containing 0.1% HTAB (wt v^{-1}), was homogenized by Ultra-Turrax (Ika-Werk, Staufen, Germany) for 5 s at 20 000 r.p.m. The homogenate was centrifuged at 15 000 g for 5 min, and the supernatant was used for the colorimetric assay, because preliminary experiments revealed that the pellet contained less than 5% of total myeloperoxidase activity. In each well of a 96-well microplate, 25 µL of the supernatant was mixed with 50 µL of the chromogen solution [2.83 mM TMB dissolved in 0.1 M sodium acetate buffer at pH 4.2, containing 0.1% (wt v^{-1}) HTAB]. The enzyme reaction was started by adding 75 µL of 0.7 mM hydrogen peroxide. After 5 min of incubation at 25°C, the reaction was blocked by 50 µL of 4 M acetic acid, containing 10 nM sodium azide. The absorbance was read at 620 nm using an automated microplate reader (Bio-Tek Instruments, Winooski, VT, USA). Myeloperoxidase activity was expressed as enzyme units in 1 mL of supernatant. One unit of peroxidase activity was defined as the amount of enzyme oxidizing 1 nmol of TMB min^{-1}. The enzyme activity of each sample was determined in duplicate.

Statistical analysis

Results are expressed as means ± SD and were analysed by Student's *t*-test; *P* values less than 0.05 were considered to be statistically significant. *In vivo* data were analysed by one-way analysis of variance followed by Dunnett's test for multiple comparisons of unpaired data, and a probability level lower than 0.05 was considered as significant. The dose giving 50% inhibition of the oedematous response (ID_{50}) was calculated by graphic interpolation of the logarithmic dose–effect curves.

Materials

Rimonabant [N-(piperidino-1-yl)-5-(4-chlorophenyl)-1-(2,4dichlorophenyl)-4-methyl-pyrazole-3-carboxamide] was kindly provided by Sanofi-Aventis (Montpellier, France) and was dissolved in dimethylsulfoxide. The vehicle did not induce any positive result in any assay. Croton oil and indomethacin were purchased from Sigma Aldrich (Milan, Italy), while ketamine hydrochloride (Inoketam100) was from Virbac (Milan, Italy).

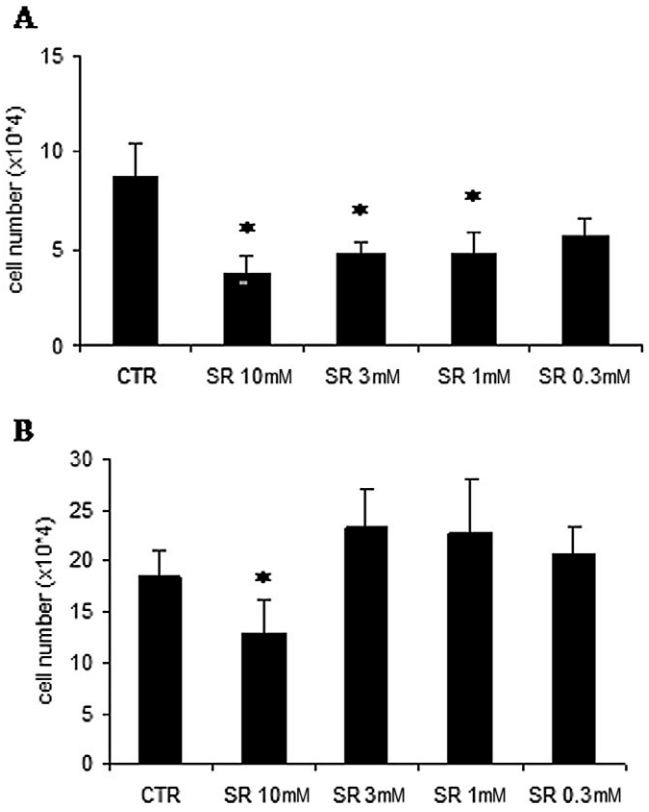

Figure 1

Rimonabant reduces C5N cell viability. C5N cells cultured in the presence and in the absence of rimonabant (SR), at the concentrations shown, were collected after 24 h (A) and 48 h (B) of treatment, stained by Trypan blue and counted by haemocytometer. Data for control (CTR) represent the effects of the vehicle. The histograms shown representative of four experiments. Data are means ± SD; * $P < 0.05$, significantly different from control values.

Results

Rimonabant reduces C5N cell viability

C5N cells were cultured in the presence and in the absence of rimonabant at increasing concentrations ranging from 0.3 μM to 10 μM. Cell survival was determined after 24 h and 48 h of treatments by Trypan blue staining and cells were counted by haemocytometer. Results obtained showed that rimonabant caused decrease of cell viability after 24 h treatment (Figure 1A). The inhibitory effect was maintained after 48 h of treatment only at the highest concentration used (Figure 1B).

Cytotoxic effects of rimonabant in C5N cells

In order to assess cell cytotoxicity following rimonabant treatment, we performed sulphorhodamine B staining. Cells were cultured in triplicates at increasing concentrations ranging from 0.3 μM to 10 μM of rimonabant and collected after 24 h of incubation, as at this time point the reduced cell viability reached its maximum. We found decreased cell survival at the highest concentrations used (Figure 2).

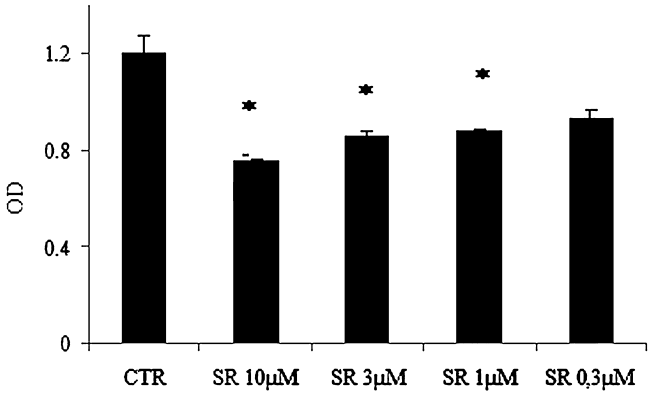

Figure 2

Cytoxicity of rimonabant. C5N cells incubated with rimonabant, at the concentrations shown, were collected after 24 h treatment and stained by sulphorhodamine B. The optical density (OD) at 495 nm was determined by a microplate reader. The histogram shown is representative of three independent experiments. Data are means ± SD; * $P < 0.05$, significantly different from control values.

Rimonabant effects on cell cycle progression

To better characterize the inhibition of cell viability by rimonabant and correlate this effect with cell cycle progression, we analysed cell cycle distribution by flow cytometry. C5N cells were cultured in DMEM + 10%FBS and treated with rimonabant at increasing concentrations ranging from 0.3 μM to 10 μM. Rimonabant enhanced the number of cells in the subG0 phase of the cell cycle in a concentration-dependent manner after 24 h of treatment (Figure 3).

Rimonabant effects on the expression levels of NF-κBp65, pNF-κBp65, IκBα, pIκBα, Bax, Bcl-2, XIAP, pAkt, Akt, Cyc D1, Cyc E, Cyc A and CB_1 receptors

In order to assess potential pathways involved in the effects of rimonabant, we analysed in cell extracts, the expression levels of NF-κBp65, pNF-κBp65, IκBα, pIκBα, pAkt and Akt. We found a reduction of the expression levels of pAkt and pNF-κBp65 following rimonabant treatment, together with no changes of total Akt, enhanced expression of both total NF-κBp65 and IκBα and pIκBα after 24 h treatment and their reduced expression after 48 h at the highest concentrations (Figure 4; Table 1).

To better characterize the effects of rimonabant on cell death we investigated the expression levels of the apoptotic cell marker, Bax and anti-apoptotic Bcl-2 and XIAP. We found enhanced expression of Bax after 24 h and 48 h treatment and reduced expression of Bcl-2 after 24 h at 10 μM more pronounced after 48 h at the highest concentrations. Reduced levels of XIAP were detected after 48 h (Figure 4; Table 1). As rimonabant modified cell cycle progression, we investigated the expression levels of various cell cycle regulatory molecules, including cyclin D1, cyclin E and cyclin A. As shown in Figure 4, treatment of cells with rimonabant increased the expression of these cyclins after 24 h in comparison to untreated cells (Table 1) but after 48 h of treatment

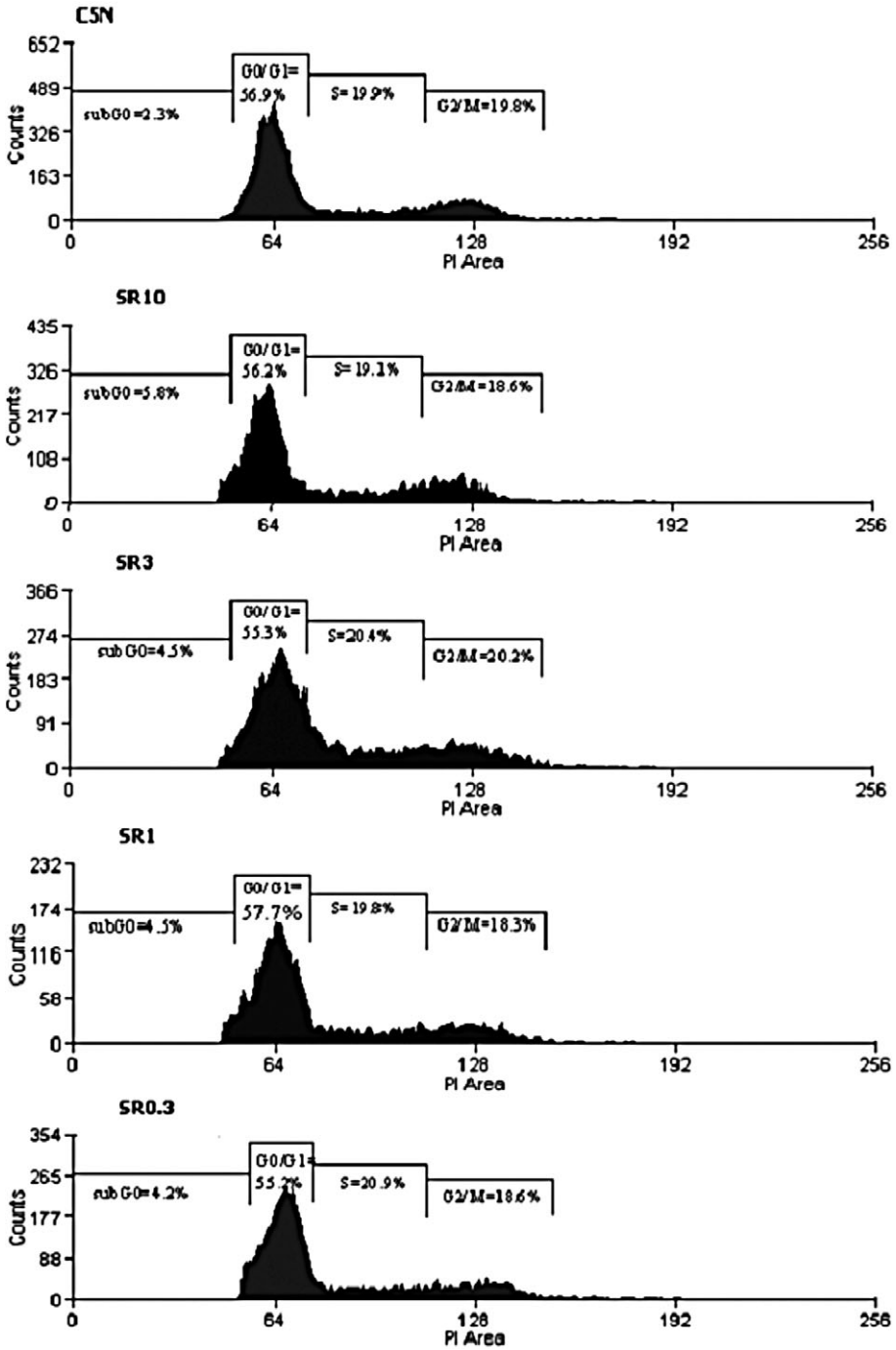

Figure 3

Rimonabant increased the proportion of cells in the subG0 phase of the cell cycle. C5N cells cultured in the presence and in absence of rimonabant (SR) at the concentration showed in the histograms, were collected after 24 h of incubation, stained with propidium iodide and analysed by flow cytometry. The cell cycle profile of a single experiment representative of three is reported in the figure. The per cent of cells in each phase of the cell cycle is shown for each histogram and represent the mean of three independent experiments.

the protein expression of cyclin D1, cyclin E and cyclin A was reduced in a dose-dependent manner.

Furthermore, we investigated potential modification of the CB_1 receptor, that is expressed in C5N cells as detected in the control (Figure 4), following treatment with the CB_1 receptor antagonist. Interestingly, we found an induction of the CB_1 receptor at all time points and concentrations of rimonabant used with respect to the untreated control cells. This effect was not maintained at 10 μM after 48 h treatment (Figure 4; Table 1).

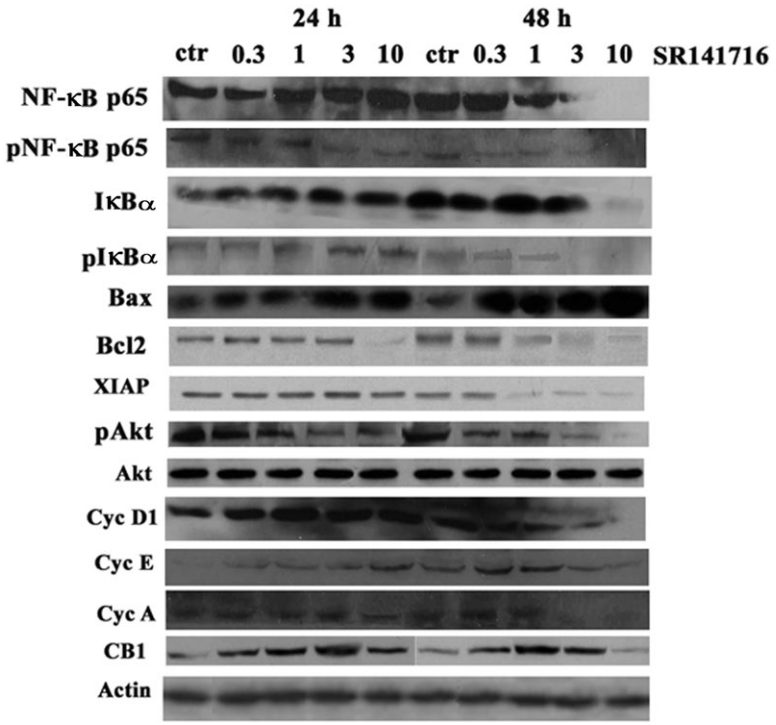

Figure 4

Effects of rimonabant on the expression levels of NF-kBp65, pNF-kBp65, IκBα, pIκBα, Bax, Bcl-2, xIAP, pAkt, Akt, Cyc D1, Cyc E, Cyc A and CB_1 receptors in C5N cells. Cell extracts obtained from cells cultured in the presence and in absence of rimonabant at 24 h and 48 h treatment, were analysed by Western blotting. The concentrations of rimonabant used are shown above the experimental records. A representative blot for NF-kBp65, pNF-kBp65, IκBα, pIκBα, Bax, Bcl-2, XIAP, pAkt, Akt, cyclins D1, E and A (Cyc D1, E and A) and CB_1 receptors (CB_1) is shown in the figure. Summary data from these experiments are shown in Table 1. IκBα, inhibitor of nuclear factor kappa B alpha; NF-κB, nuclear factor kappa B, pNF-κB, phosphorylated NF-κB; pIκBα, phosphorylated IκBα; XIAP, X-inhibitor of apoptosis protein.

Topical anti-inflammatory actions of rimonabant in vivo

The topical anti-inflammatory activity of rimonabant was evaluated as inhibition of the croton oil-induced ear dermatitis in mice in comparison with that of the NSAID indomethacin. After 6 h, when oedema formation in control mice is maximum (Tubaro *et al.*, 1985), rimonabant induced a dose-dependent reduction of oedema (Table 2). At the same doses, indomethacin also reduced the oedematous response. The anti-oedema potency of the two compounds was assessed from the dose–response curves, calculating the relevant ID_{50} values. The ID_{50} of rimonabant was 0.34 μmol·cm^{-2}, showing a potency comparable to that of the reference NSAID indomethacin (ID_{50} = 0.26 μmol·cm^{-2}) (Table 2). The anti-inflammatory activity of an equimolar dose of rimonabant and indomethacin (0.3 μmol·cm^{-2}) was further evaluated on both oedema and leukocyte infiltrate, at the times of their maximum in control mice (6 h and 24 h respectively) (Tubaro *et al.*, 1985). Six hours and 24 h after induction of inflammation, rimonabant reduced oedema and indomethacin exerted a similar effect after 6 h but no effect after 24 h (Table 3). Rimonabant also significantly reduced also the recruitment of neutrophilic granulocytes in the ear tissue: at 6 h and 24 h (Table 4). The reference compound, indomethacin, exerted a comparable effect at 6 h and 24 h after the dermatitis induction (Table 4).

Discussion and conclusions

In this study we assessed the effects of the CB_1 receptor antagonist, rimonabant (Rinaldi-Carmona *et al.*, 1994) *in vitro*, in a murine-immortalized keratinocyte cell line and *in vivo*, in a model of skin inflammation to evaluate potential anti-inflammatory properties of this drug related to epidermal dysfunction. We observed that rimonabant reduced C5N cell viability and induced apoptosis as showed by the enhanced level of Bax, reduction of Bcl-2 and XIAP and the increased number of cells in the subG0 phase of the cell cycle. Previous reports had demonstrated that cannabinoids inhibited proliferation of epidermal keratinocytes (Ibrahim *et al.*, 2005; Wilkinson and Williamson, 2007; Paradisi *et al.*, 2008), hair matrix keratinocytes (Telek *et al.*, 2007; Dobrosi *et al.*, 2008) and induced intraepithelial apoptosis and premature regression of hair follicles. A fundamental role of NF-κB has been described in apoptosis and inhibition of the NF-κB action in TNFα-stimulated keratinocytes showed significant apoptosis (Banno *et al.*, 2005). In addition, NF-κB blocked apoptosis by induction of anti-apoptotic genes, such as the Bcl-2 homologs and IAPs (Hu *et al.*, 1998; Zong *et al.*, 1999; Chen *et al.*, 2000). In agreement with this finding, we detected down-regulation of XIAP, reduction of pNF-κBp65, associated with enhanced expression of pIκBα, total NF-κB and IκB at early time points and reduced levels at late time

Table 1

Effects of rimonabant (SR; 0.3–10 μM) on NF-κB, components of apoptosis, cyclins (Cyc) and CB_1 receptor (CB1) proteins in C5N keratinocytes

	24 h ctr	SR 0.3	SR 1	SR 3	SR 10	48 h ctr	SR 0.3	SR 1	SR 3	SR 10
NF-κB	1.2	1	2*	2*	4*	4	4	1*	0.5*	0*
pNF-κB	1	0.8*	0.8*	0.5*	0.5*	0.8	0.4	0.5*	0.25*	0*
IκBα	0.5	1	1.5*	2*	2*	3	2.8*	3.3*	3*	0.01*
pIκBα	0.5	0.5	0.6*	1*	1*	0.5	0.5	0.3*	0*	0*
Bax	1	2	2*	4*	4*	0.7	4	4*	4*	4*
Bcl-2	0.95	1	1*	1*	0.1*	1.5	1.3	0.5*	0.25*	0.1*
XIAP	1	1	1*	1.2*	0.95*	0.85	0.8	0.3*	0.35*	0.2*
pAkt	2	1.5	1*	0.5*	0.57*	2	0.8	1*	0.4*	0.01*
Akt	2	2	2*	2*	2*	2	2	2*	2*	2*
Cyc D1	1	2	3*	3*	3*	2	1	1*	0.5*	0*
Cyc E	0	0.5	0.5*	0.6*	1*	0.9	1.5	1.2*	0.5*	0.2*
Cyc A	0.5	0.5	0.6*	0.75*	0.75*	0.8	1	0.9*	0*	0*
CB1	0.5	1	1.5*	2*	1*	0.5	0.95	2*	1.5*	0.6*

Cell extracts were analysed by Western blotting (as illustrated in Figure 4) after 24 h and also after 48 h incubation with rimonabant. Immunoreactive bands were quantified with the Quantity One programme. The table shows quantification of the intensity of bands (as means; $n = 3$), normalized to the intensity of the actin bands.

*$P < 0.05$, significantly different from corresponding control (ctr); Student's *t*-test.

IκBα, inhibitor of nuclear factor kappa B alpha; NF-κB, nuclear factor kappa B, pNF-κB, phosphorylated NF-κB; pIκBα, phosphorylated IκBα; XIAP, X-inhibitor of apoptosis protein.

Table 2

Dose-dependent anti-oedema activity of rimonabant and indomethacin in croton oil-induced ear dermatitis after 6 h

Substance	Number of mice	Dose (μmol·cm^{-2})	Oedema (mg) Mean ± SD	% reduction	ID_{50} (μmol·cm^{-2})
Controls	10	–	7.0 ± 1.0	–	–
Rimonabant	10	0.1	5.3 ± 0.6*	24	0.34
	10	0.3	3.4 ± 0.6**	51	
	10	1.0	2.1 ± 0.7**	70	
Indomethacin	10	0.1	5.2 ± 0.4*	26	0.26
	10	0.3	3.0 ± 0.4**	57	
	10	1.0	1.4 ± 0.3**	80	

*$P < 0.005$, **$P < 0.001$, significantly different from control values; one-way ANOVA.

points likely due to degradation effects at the highest concentration of rimonabant. Evidence showing inhibition of pAkt related to induction of apoptotic pathways (Kumar *et al.*, 2009), support our finding demonstrating that rimonabant down-regulates pAkt while no effect was observed on total Akt. Cyclin D1 has been described as a direct NF-κB target gene in several cell types (Hinz *et al.*, 1999), TNF-α increased the binding of NF-κB proteins to the κB site on the cyclin D1 promoter (Zhang *et al.*, 2007), indeed NF-κB activation was essential for induction of cyclin D1 (Schmidt-Ullrich *et al.*, 2006). We detected concomitant accumulation of NF-κB and induction of cyclin D1, after 48 h at the highest concentration of rimonabant. The decreased levels of NF-κB were accompanied by reduced expression of cyclin D1, similar effects we observed in the levels of cyclin A and E. Interestingly, we found that rimonabant enhanced considerably the levels of CB_1 receptors and that this effect was lost at the highest concentration after 48 h of treatment, probably due to the longer time of incubation of the antagonist and sequestration of its receptor. However, even if we found up-regulation of CB_1 receptors, the effects of rimonabant that we observed might not be mediated by these receptors. Further studies are needed to determine if the action of rimonabant is due to CB_1 receptor blockade. Several studies

Table 3

Effect of rimonabant and indomethacin on the oedematous response in croton oil-induced ear dermatitis after 6 h and 24 h

Substance	Number of mice	Dose (μmol cm^2-1)	6 h Oedema (mg) mean ± SD	% reduction	24 h Oedema (mg) mean ± SD	% reduction
Controls	10	–	7.0 ± 0.8	–	2.3 ± 0.6	–
Rimonabant	10	0.3	3.0 ± 0.6**	57	1.2 ± 0.4*	48
Indomethacin	10	0.3	2.7 ± 0.9**	61	2.2 ± 0.6	4

*P < 0.005, **P < 0.001, significantly different from control values; one-way ANOVA.

Table 4

Effect of rimonabant and indomethacin on the leukocyte infiltrate in croton oil-induced ear dermatitis after 6 h and 24 h

Substance	Number of mice	Dose (μmol·cm^{-2})	6 h MPO (EU) mean ± SD	% reduction	24 h MPO (EU) mean ± SD	% reduction
Controls	10	–	18.6 ± 1.9	–	30.5 ± 4.5	–
Rimonabant	10	0.3	13.0 ± 1.8*	30	22.2 ± 2.1*	27
Indomethacin	10	0.3	11.7 ± 1.4*	37	20.6 ± 4.7*	32

*P < 0.005, significantly different from control values; one-way ANOVA.
MPO, myeloperoxidase; EU, enzyme units (nmol tetramethylbenzidine hydrolysed min^{-1}).

demonstrated antinociceptive properties of locally administered cannabinoids in animal models (Hohmann, 2002; Walker and Huang, 2002; Mbvudula *et al.*, 2004) and these effects were dependent on CB_1 receptors (Agarwal *et al.*, 2007). CB_1 receptor-mediated antinociception has been attributed to activation of CB_1 receptors (Ahluwalia *et al.*, 2000; Ständer *et al.*, 2005; Amaya *et al.*, 2006), indeed stimulation of cannabinoid receptors reduced contact allergic inflammation (Karsak *et al.*, 2007). Rimonabant has been proved to be a strong anti-inflammatory agent (Costa, 2007), attenuating weight gain in Zucker rats, lowering neutrophil and monocyte counts, platelet activation and aggregation and circulating pro-inflammatory cytokine levels (Di Marzo and Szallasi 2008). However, it is still not clear if the anti-inflammatory actions of rimonabant are mediated by CB_1 receptors and due to antagonist, or more likely, to inverse agonist effects (Karsak *et al.*, 2007).

Recently, the vanilloid receptor (TRPV1) was also proposed to be involved in contact allergic dermatitis, as there was up-regulation of TRPV1 receptors and palmitoyl ethanolamide levels in ear keratinocytes. Also, palmitoyl ethanolamide inhibited ear inflammation in mice *in vivo*, and this inhibition was attenuated by antagonism at TRPV1 receptors (Petrosino *et al.*, 2010). In the model of acute inflammation used here, croton oil-induced ear dermatitis in mice (Tubaro *et al.*, 1985), we found that rimonabant exhibited a dose-dependent anti-oedema activity comparable to that of the NSAID indomethacin at 6 h after dermatitis induction. Rimonabant was still active after 24 h, when indomethacin had lost its anti-oedema effect, as previously reported (Tubaro *et al.*, 1985; Giangaspero *et al.*, 2009). Moreover, rimonabant significantly reduced the leukocyte infiltrate, as did the equimolar dose of indomethacin.

Our findings showed that rimonabant reduced cell viability, was cytotoxic, induced apoptosis in C5N keratinocytes by regulation of Akt, NF-κB, IκBα pathways, cyclins D1, E and A and up-regulated CB_1 receptors. We have provided evidence that the apoptotic effect *in vitro* is related to anti-inflammatory properties *in vivo*. The finding that rimonabant decreased croton oil-induced ear dermatitis in mice suggests a potential therapeutic application of the CB_1 receptor antagonist as a topical anti-inflammatory drug.

Acknowledgements

This work was supported by Sanofi-Aventis (M.B.) and Associazione Educazione e Ricerca Medica Salernitana (ERMES).

Conflicts of interest

None.

References

Agarwal N, Pacher P, Tegeder I, Amaya F, Constantin CE, Brenner GJ *et al.* (2007). Cannabinoids mediate analgesia largely via peripheral type 1 cannabinoid receptors in nociceptors. Nat Neurosci 10: 870–879.

Alexander SPH, Mathie A, Peters JA (2009). Guide to Receptors and Channels (GRAC), 4th edition. Br J Pharmacol 158 (Suppl. 1), S1–S254.

Ahluwalia J, Urban L, Capogna M, Bevan S, Nagy I (2000).Cannabinoid 1 receptors are expressed in nociceptive primary afferent sensory neurons. Neuroscience 100: 685–688.

Amaya F, Shimosato G, Kawasaki Y, Hashimoto S, Tanaka Y, Ji RR *et al.* (2006). Induction of CB1 cannabinoid receptor by inflammation in primary afferent neurons facilitates antihyperalgesic effect of peripheral CB1 agonist. Pain 124: 175–183.

Andrews PC, Krinsky NI (1981). The reductive cleavage of myeloperoxidase in half, producing enzymatically active hemi-peroxidase. J Biol Chem 256: 4211–4218.

Aquila S, Guido C, Santoro A, Gazzerro P, Laezza C, Baffa MF, Andò S, Bifulco M. (2010). Rimonabant (SR141716) induces metabolism and acquisition of fertilizing ability in human sperm. Br J Pharmacol 159: 831–841.

Banno T, Gazel A, Blumenberg M (2005). Pathway-specific profiling identifies the NF-kappa B-dependent tumor necrosis factor alpha-regulated genes in epidermal keratinocytes. J Biol Chem 280: 18973–18980.

Bradford MM. (1976). A rapid and sensitive method for the quantitation of microgram quantities of protein utilizing the principle of protein-dye binding. Anal Biochem 72: 248–254.

Bradley PP, Priebat DA, Christensen RD, Rothstein G (1982). Measurement of cutaneous inflammation: estimation of neutrophil content with an enzyme marker. J Invest Dermatol 78: 206–209.

Carai MA, Colombo G, Gessa GL (2005). Rimonabant: the first therapeutically relevant cannabinoid antagonist. Life Sci 77: 2339–2350.

Chen C, Edelstein LC, Gelinas C (2000). The Rel/NF-kB family directly activates expression of the apoptosis inhibitor Bcl-x(L). Mol Cell Biol 20: 2687–2695.

Colombo G, Agabio R, Diaz G, Lobina C, Reali R, Gessa GL (1998). Appetite suppression and weight loss after the cannabinoid antagonist SR 141716. Life Sci 63: PL113–PL117.

Costa B (2007). Rimonabant: more than an anti-obesity drug? Br J Pharmacol 150: 535–537.

Costa B, Trovato AE, Colleoni M, Giagnoni G, Zarini E, Croci T (2005). Effect of the cannabinoid CB1 receptor antagonist, SR141716, on nociceptive response and nerve demyelination in rodents with chronic constriction injury of the sciatic nerve. Pain 116: 52–61.

Croci T, Zarini E (2007). Effect of the cannabinoid CB1 receptor antagonist rimonabant on nociceptive responses and adjuvantinduced arthritis in obese and lean rats. Br J Pharmacol 150: 559–566.

Croci T, Landi M, Galzin AM, Marini P (2003). Role of cannabinoid CB1 receptors and tumor necrosis factor-alpha in the gut and systemic anti-inflammatory activity of SR 141716 (rimonabant) in rodents. Br J Pharmacol 140: 115–122.

Di Marzo V, Matias I (2005). Endocannabinoid control of food intake and energy balance. Nat Neurosci 8: 585–589.

Di Marzo V, Szallasi A. (2008). Rimonabant in rats with a metabolic syndrome: good news after the depression. Br J Pharmacol 154: 915–917.

Dobrosi N, Tóth BI, Nagy G, Dózsa A, Géczy T, Nagy L *et al.* (2008). Endocannabinoids enhance lipid synthesis and apoptosis of human sebocytes via cannabinoid receptor-2-mediated signaling. FASEB J 22: 3685–3695.

Engeli S, Bohnke J, Feldpausch M, Gorzelniak K, Janke J, Batkai S *et al.* (2005). Activation of the peripheral endocannabinoid system in human obesity. Diabetes 54: 2838–2843.

Gazzerro P, Malfitano AM, Proto MC, Santoro A, Pisanti S, Caruso MG *et al.* (2010). Synergistic inhibition of human colon cancer cell growth by the cannabinoid CB1 receptor antagonist rimonabant and oxaliplatin Oncol Rep 23: 171–175.

Giangaspero A, Ponti C, Pollastro F, Del Favero G, Della Loggia R, Tubaro A, Appendino G, Sosa, S (2009). Topical anti-inflammatory activity of eupatilin, a lipophilic flavonoid from mountain wormwood (*Artemisia umbelliformis* Lam.). J Agric Food Chem 57: 7726–7730.

Guindon J, Hohmann AG. (2008). Cannabinoid CB2 receptors: a therapeutic target for the treatment of inflammatory and neuropathic pain. Br J Pharmacol 153: 319–334.

Hinz M, Krappmann D, Eichten A, Heder A, Scheidereit C, Strauss M (1999). NF-κB function in growth control: regulation of cyclin D1 expression and G0/G1-to-S-phase transition. Mol Cell Biol 19: 2690–2698.

Hohmann AG (2002).Spinal and peripheral mechanisms of cannabinoid antinociception: behavioral, neurophysiological and neuroanatomical perspectives. Chem Phys Lipids 121: 173–190.

Hu X, Yee E, Harlan JM, Wong F, Karsan A (1998). Lipopolysaccharide induces the antiapoptotic molecules, A1 and A20, in microvascular endothelial cells. Blood 92: 2759 –2765.

Ibrahim MM, Porreca F, Lai J, Albrecht PJ, Rice FL, Khodorova A *et al.* (2005). CB2 cannabinoid receptor activation produces antinociception by stimulating peripheral release of endogenous opioids. Proc Natl Acad Sci U S A. 102: 3093–3098.

Jbilo O, Ravinet-Trillou C, Arnone M, Buisson I, Bribes E, Peleraux A *et al.* (2005). The CB1 receptor antagonist rimonabant reverses the diet-induced obesity phenotype through the regulation of lipolysis and energy balance. FASEB J 19: 1567–1569.

Jhaveri MD, Richardson D, Chapman V (2007). Endocannabinoid metabolism and uptake: novel targets for neuropathic and inflammatory pain. Br J Pharmacol 152: 624–632.

Karsak M, Gaffal E, Date R, Wang-Eckhardt L, Rehnelt J, Petrosino S, *et al.* (2007). Attenuation of allergic contact dermatitis through the endocannabinoid system. Science 316: 1494–1497.

Kumar S, Bryant CS, Chamala S, Qazi A, Seward S, Pal J *et al.* (2009). Ritonavir blocks AKT signaling, activates apoptosis and inhibits migration and invasion in ovarian cancer cells. Mol Cancer 8: 26.

Maccarrone M, Di Rienzo M, Battista N, Gasperi V, Guerrieri P, Rossi A *et al.* (2003). The endocannabinoid system in human keratinocytes. Evidence that anandamide inhibits epidermal differentiation through CB1 receptordependent inhibition of protein kinase C, activation protein-1, and transglutaminase. J Biol Chem 278: 33896–33903.

Malfitano AM, Laezza C, Pisanti S, Gazzerro P, Bifulco M (2008). Rimonabant (SR141716) exerts anti-proliferative and immunomodulatory effects in human peripheral blood mononuclear cells. Br J Pharmacol 153: 1003–1010.

Matias I, Gonthier MP, Orlando P, Martiadis V, De Petrocellis L, Cervino C *et al.* (2006). Regulation, function, and dysregulation of endocannabinoids in models of adipose and beta-pancreatic cells and in obesity and hyperglycemia. J Clin Endocrinol Metab 91: 3171–3180.

Mbvudula EC, Rainsford KD, Bunning RAD (2004). Cannabinoids in pain and inflammation. Inflammopharmacology 12: 99–114.

Miller AM, Stella N (2008). CB2 receptor-mediated migration of immune cells: it can go either way. Br J Pharmacol 153: 299–308.

Paradisi A, Pasquariello N, Barcaroli D, Maccarrone M (2008). Ananamide regulates keratinocyte differentiation by inducing DNA methylation in a CB1 receptor-dependent manner. J Biol Chem 283: 6005–6012.

Pertwee RG (2009). Emerging strategies for exploiting cannabinoid receptor agonists as medicines. Br J Pharmacol 156: 397–411.

Petrosino S, Cristino L, Karsak M, Gaffal E, Ueda N, Tüting T *et al.* (2010). Protective role of palmitoylethanolamide in contact allergic dermatitis. Allergy 65: 698–711

Portella G, Cumming SA, Liddell J, Cui W, Ireland H, Akhurst RJ *et al.* (1998) Transforming growth factor beta is essential for spindle cell conversion of mouse skin carcinoma *in vivo*: implications for tumor invasion. Cell Growth Differ 9: 393–404.

Ravinet Trillou C, Arnone M, Delgorge C, Gonalons N, Keane P, Maffrand JP *et al.* (2003). Anti-obesity effect of SR 141716, a CB1 receptor antagonist, in diet-induced obese mice. Am J Physiol Regul Integr Comp Physiol 284: R345–R353.

Rinaldi-Carmona M, Barth F, Héaulme M, Shire D, Calandra B, Congy C *et al.* (1994). SR141716A, a potent and selective antagonist of the brain cannabinoid receptor. FEBS Lett 350: 240–244.

Rinaldi-Carmona M, Barth F, Héaulme M, Alonso R, Shire D, Congy C *et al.* (1995). Biochemical and pharmacological characterisation of SR 141716A, the first potent and selective brain cannabinoid receptor antagonist. Life Sci 56: 1941–1947.

Santoro A, Gazzerro P, Malfitano AM, Pisanti S, Laezza C, Bifulco M (2008). Reply to the letter to the editor 'Long-term cannabinoid receptor (CB1) blockade in obesity: implications for the development of colorectal cancer'. Int J Cancer 123: 243–244.

Santoro A, Pisanti S, Grimaldi C, Izzo A, Borrelli F, Proto MC *et al.* (2009). Rimonabant inhibits human colon cancer cell growth and reduces the formation of precancerous lesions in the mouse colon. Int J Cancer 125: 996–1003.

Sarnataro D, Pisanti S, Santoro A, Gazzerro P, Malfitano AM, Laezza C *et al.* (2006). The cannabinoid CB1 receptor antagonist rimonabant (SR141716) inhibits human breast cancer cell proliferation through a lipid rafts mediated mechanism. Mol Pharmacol 70: 1298–1306.

Schmidt-Ullrich R, Tobin DJ, Lenhard D, Schneider P, Paus R, Scheidereit C (2006). NF-kappaB transmits Eda A1/EdaR signalling to activate Shh and cyclin D1 expression, and controls post-initiation hair placode down growth. Development 133: 1045–1057.

Simiand J, Keane M, Keane PE, Soubrié P (1998). SR 141716, a CB1 cannabinoid receptor antagonist, selectively reduces sweet food intake in marmoset. Behav Pharmacol 9: 179–181.

Smith SR, Terminelli C, Denhardt G (2000). Effects of cannabinoid receptor agonist and antagonist ligands on production of inflammatory cytokines and anti-inflammatory interleukin-10 in endotoxemic mice. J Pharmacol Exp Ther 293: 136–150.

Ständer S, Schmelz M, Metze D, Luger T, Rukwied R (2005). Distribution of cannabinoid receptor 1 (CB1) and 2 (CB2) on sensory nerve fibers and adnexal structures in human skin. J Dermatol Sci 38: 177–188.

Telek A, Bíró T, Bodó E, Tóth BI, Borbíró I, Kunos G *et al.* (2007). Inhibition of human hair follicle growth by endo- and exocannabinoids. FASEB J 21: 3534–3541.

Tubaro A, Dri, P, Delbello G, Zilli C, Della Loggia R (1985). The Croton oil ear test revisited. Agents Actions 17: 347–349.

Walker JM, Huang SM (2002).Cannabinoid analgesia. Pharmacol Therapeut 95: 127–135.

Wilkinson JD, Williamson EM (2007). Cannabinoids inhibit human keratinocyte proliferation through a non-CB1/CB2 mechanism and have a potential therapeutic value in the treatment of psoriasis. J Dermatol Sci 45: 87–92.

Zhang J, Warren MA, Shoemaker SF, Ip MM (2007). NFkappaB1/p50 is not required for tumor necrosis factor-stimulated growth of primary mammary epithelial cells: implications for NFkappaB2/p52 and RelB. Endocrinology 148: 268–278.

Zong WX, Edelstein LC, Chen C, Bash J, Gelinas C (1999). The prosurvival Bcl-2 homolog Bfl-1/A1 is a direct transcriptional target of NF-kB that blocks TNFa-induced apoptosis. Genes Dev 13: 382–387.